



Publication Year	2021
Acceptance in OA	2025-02-07T16:00:45Z
Title	The XMM-SERVS Survey: XMM-Newton Point-source Catalogs for the W-CDF-S and ELAIS-S1 Fields
Authors	Ni, Qingling, Brandt, W. N., Chen, Chien-Ting, Luo, Bin, Nyland, Kristina, Yang, Guang, Zou, Fan, Aird, James, Alexander, David M., Bauer, Franz Erik, Lacy, Mark, Lehmer, Bret D., Mallick, Labani, Salvato, Mara, Schneider, Donald P., TOZZI, Paolo, Traulsen, Iris, VACCARI, MATTIA, VIGNALI, CRISTIAN, VITO, Fabio, Xue, Yongquan, Banerji, Manda, Chow, Kate, COMASTRI, Andrea, Del Moro, Agnese, GILLI, Roberto, Mullaney, James, Paolillo, Maurizio, Schwope, Axel, Shemmer, Ohad, Sun, Mouyuan, Timlin, John D., III, Trump, Jonathan R.
Publisher's version (DOI)	10.3847/1538-4365/ac0dc6
Handle	http://hdl.handle.net/20.500.12386/35855
Journal	THE ASTROPHYSICAL JOURNAL SUPPLEMENT SERIES
Volume	256

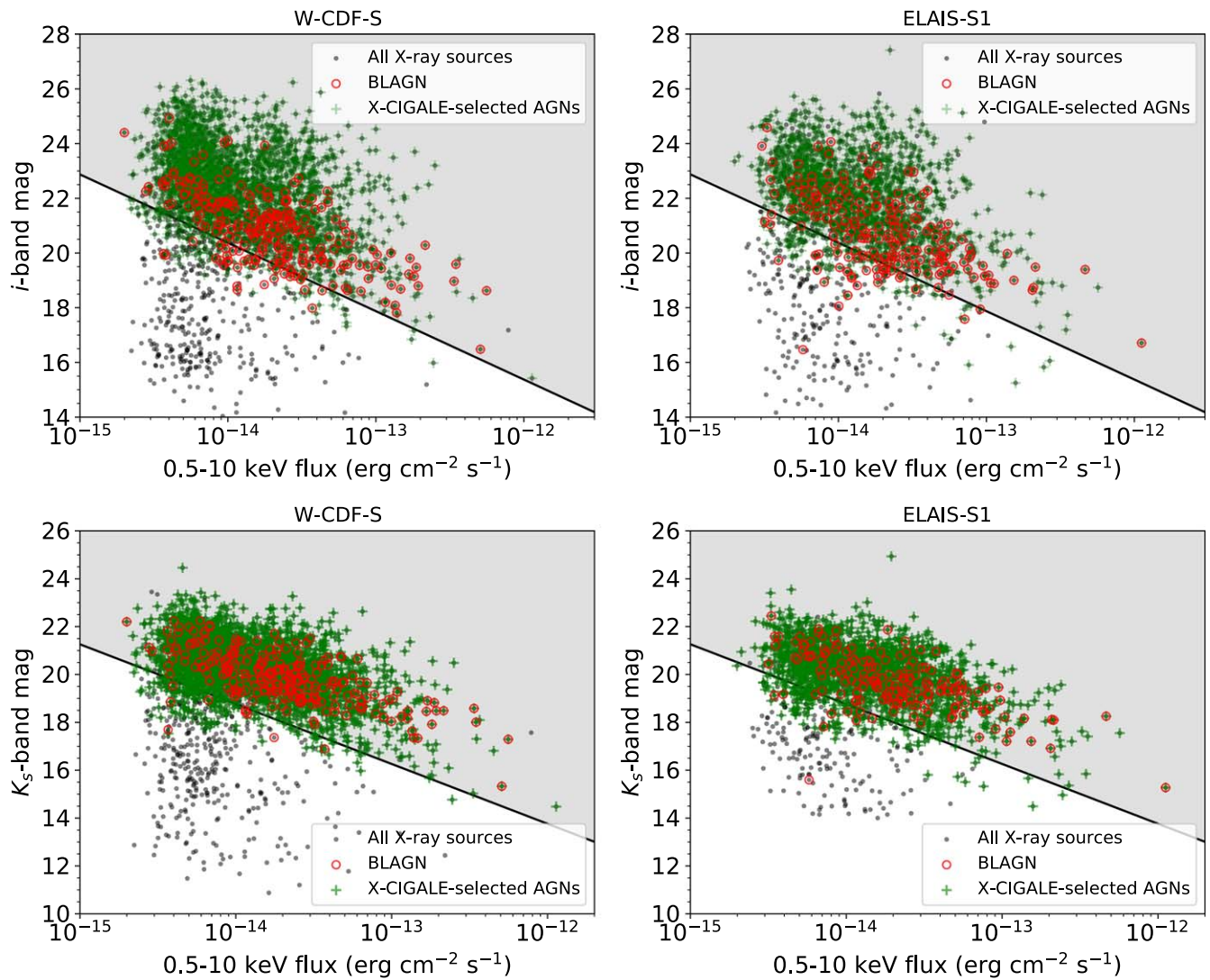


Figure 28. Left/right: HSC (or DES) *i*-band/VIDEO K_s -band magnitude vs. X-ray flux in the full band for all the X-ray sources detected in the *i*/ K_s band (black circles), *i*/ K_s -band-detected BL AGNs (red circles), and *i*/ K_s -band-detected X-ray sources that are classified as AGNs from X-CIGALE SED fitting (green plus signs) in W-CDF-S (top panels) and ELAIS-S1 (bottom panels). The shaded region marks the “AGN region” defined by the $\log_{10} f_x / f_i > -1$ or $\log_{10} f_x / f_{K_s} > -1.2$ threshold (represented by the black solid line).

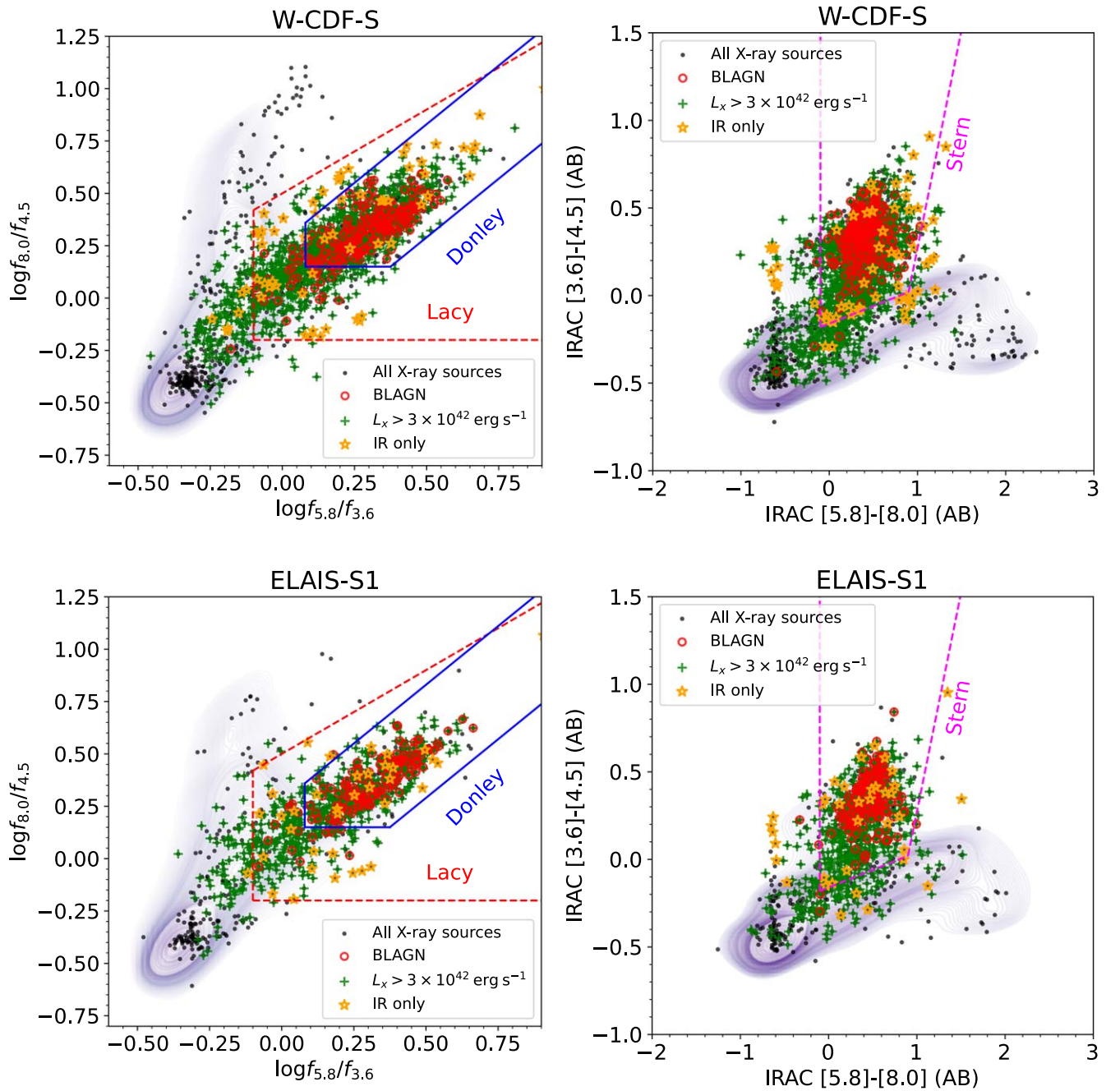


Figure 29. Left panels: the distribution of $\log f_{5.8}/f_{3.6}$ vs. $\log f_{8.0}/f_{4.5}$ for X-ray sources that are detected in four IRAC bands (black circles), with the 2D kernel density plot of all SWIRE sources detected in four IRAC bands in the background in W-CDF-S (top) and ELAIS-S1 (bottom). Among these X-ray sources, BL AGNs are marked by the red circles, AGNs identified with high L_x values are marked by green plus signs, and X-ray sources that are only identified as AGN via MIR colors are marked by orange stars. The blue lines denote the Donley wedge (Donley et al. 2012); the red dashed lines denote the Lacy wedge (Lacy et al. 2004). Right panels: the distribution of IRAC [5.8] – [8.0] vs. [3.6] – [4.5] (AB) for all X-ray sources that are detected in four IRAC bands (black circles), with the 2D kernel density plot of all SWIRE sources detected in four IRAC bands in the background in W-CDF-S (top) and ELAIS-S1 (bottom). Symbols represent the same objects as in the left panel. The magenta dashed lines denote the Stern wedge (Stern et al. 2005).

Appendix A

Main X-Ray Source Catalog Description

The descriptions of the columns included in our main X-ray source catalogs in W-CDF-S and ELAIS-S1 (see Tables 6 and 7) are presented below in a format similar to that of Chen et al. (2018). Throughout the table, null values are set to -99 . All celestial coordinates are given in equinox J2000.

Table 6: X-ray source catalog in W-CDF-S

X-ray properties

Columns (1)–(110) list the X-ray properties of our sources. Columns for the soft/hard/full-band results are marked with the “SB_”/“HB_”/“FB_” prefix.

1. Column (1), XID: the source ID of each X-ray source.
2. Columns (2)–(3), RA, DEC: R.A. and decl. (in degrees) of the X-ray source. Based on availability, we use the

Table 6
The Main X-Ray Source Catalog in W-CDF-S with a Selection of Columns

XID (1)	R.A. (2)	Decl. (3)	XPOSERR (4)	FB_EXP (19)	FB_BKG (31)	FB_SCTS (43)	0p5_10_FLUX (104)	SPECZ (189)	AGN_FLAG (206)
WCDFS0000	52.152070	-28.698755	0.14	90110.6	3.78	8505.6	1.13635	0.10870	1
WCDFS0001	52.168228	-28.669922	0.29	118105.5	4.87	1948.1	0.05208	0.77247	1
WCDFS0002	52.130722	-28.880466	0.30	64600.6	3.95	1917.3	0.11816	1.04995	1
WCDFS0003	52.136161	-28.733398	0.33	100678.1	4.05	1555.2	0.04719	-99	1
WCDFS0004	51.876881	-28.512461	0.34	99457.5	3.23	1430.5	0.05912	0.38893	1

(This table is available in its entirety in machine-readable form.)

Table 7
The Main X-Ray Source Catalog in ELAIS-S1 with a Selection of Columns

XID (1)	R.A. (2)	Decl. (3)	XPOSERR (4)	FB_EXP (19)	FB_BKG (31)	FB_SCTS (43)	0p5_10_FLUX (104)	SPECZ (180)	AGN_FLAG (197)
ES0000	8.747565	-44.824939	0.13	42850.9	1.96	5539.8	0.56817	-99.0	1
ES0001	8.726280	-44.771419	0.16	52141.0	2.00	3727.6	0.32483	0.40723	1
ES0002	9.324548	-44.503995	0.21	118323.1	5.71	2356.2	0.11067	1.32429	1
ES0003	9.087287	-44.144419	0.23	58336.4	2.29	2011.9	0.23091	0.20828	1
ES0004	8.787302	-44.310709	0.25	70255.8	1.81	1770.0	0.13339	0.34187	1

(This table is available in its entirety in machine-readable form.)

positions from, in priority order, the full band, soft band, and hard band as the primary position. Band-specific positions are listed in Columns (8)–(13).

- Column (4), XPOSERR: X-ray positional uncertainty (σ_x) in arcseconds (reported with the same priority order as that of positions).
- Columns (5)–(6), R68, R99: 68% and 99.73% X-ray positional uncertainties in arcseconds based on the Rayleigh distribution (see Section 3.4).
- Column (7), EMLERR: Positional uncertainties calculated by EMLDETECT, σ_{eml} , in arcseconds (with the same priority order as that of positions).
- Columns (8)–(13), SB_RA, SB_DEC, HB_RA, HB_DEC, FB_RA, FB_DEC: R.A. and decl. (in degrees) of the source in the soft, hard, and full bands, respectively.
- Columns (14)–(16), SB_DET_ML, HB_DET_ML, FB_DET_ML: the EMLDETECT source detection likelihood in each band.
- Columns (17)–(19), SB_EXP, HB_EXP, FB_EXP: total (PN + MOS1 + MOS2) exposure time in seconds in each band.
- Columns (20)–(28), SB_EXPPN, SB_EXPM1, SB_EXPM2, HB_EXPPN, HB_EXPM1, HB_EXPM2, FB_EXPPN, FB_EXPM1, FB_EXPM2: PN, MOS1, and MOS2 exposure times in seconds in each band.
- Columns (29)–(31), SB_BKG, HB_BKG, FB_BKG: total background-map values (PN + MOS1 + MOS2) in counts per pixel in each band.
- Columns (32)–(40), SB_BKGP, SB_BKGM1, SB_BKGM2, HB_BKGP, HB_BKGM1, HB_BKGM2, FB_BKGP, FB_BKGM1, FB_BKGM2: PN, MOS1, and MOS2 background-map values in counts per pixel in each band.
- Columns (41)–(43), SB_SCTS, HB_SCTS, FB_SCTS: total (PN + MOS1 + MOS2) net counts in each band.
- Columns (44)–(52), SB_SCTSPN, SB_SCTSM1, SB_SCTSM2, HB_SCTSPN, HB_SCTSM1, HB_SCTSM2,

FB_SCTSPN, FB_SCTSM1, FB_SCTSM2: PN, MOS1, and MOS2 net counts in each band.

- Columns (53)–(64), SB_SCTS_ERR, HB_SCTS_ERR, FB_SCTS_ERR, SB_SCTSPN_ERR, SB_SCTSM1_ERR, SB_SCTSM2_ERR, HB_SCTSPN_ERR, HB_SCTSM1_ERR, HB_SCTSM2_ERR, FB_SCTSPN_ERR, FB_SCTSM1_ERR, FB_SCTSM2_ERR: uncertainties of total, PN, MOS1, and MOS2 net counts in each band reported in EMLDETECT.
- Columns (65)–(76), SB_RATE, HB_RATE, FB_RATE, SB_RATEPN, SB_RATEM1, SB_RATEM2, HB_RATEPN, HB_RATEM1, HB_RATEM2, FB_RATEPN, FB_RATEM1, FB_RATEM2: total, PN, MOS1, and MOS2 net count rates in each band, in counts s^{-1} .
- Columns (77)–(88), SB_RATE_ERR, HB_RATE_ERR, FB_RATE_ERR, SB_RATEPN_ERR, SB_RATEM1_ERR, SB_RATEM2_ERR, HB_RATEPN_ERR, HB_RATEM1_ERR, HB_RATEM2_ERR, FB_RATEPN_ERR, FB_RATEM1_ERR, FB_RATEM2_ERR: uncertainties of total, PN, MOS1, and MOS2 net count rates in each band, in counts s^{-1} .
- Columns (89)–(96), BR, BR_ERR, BRPN, BRPN_ERR, BRM1, BRM1_ERR, BRM2, BRM2_ERR: total hard-to-soft-band ratio and its uncertainty, and the hard-to-soft-band ratio and its uncertainty for each EPIC detector.
- Columns (97)–(98), HR, HR_ERR: hardness ratio and its uncertainty.
- Column (99), GAMMA: the effective power-law photon index, Γ_{eff} , derived for each source based on the hard-to-soft-band ratio.
- Columns (100)–(105), 0p5_2_FLUX, 0p5_2_FLUX_ERR, 2_10_FLUX, 2_10_FLUX_ERR, 0p5_10_FLUX, 0p5_10_FLUX_ERR: observed flux and flux uncertainty in the 0.5–2 keV, 2–10 keV, and 0.5–10 keV bands, in 10^{-12} erg $\text{cm}^{-2} \text{s}^{-1}$, after correcting for Galactic absorption. The